A MULTI-FREQUENCY FMCW GBSAR: SYSTEM DESCRIPTION AND FIRST RESULTS

Adrià Amézaga [,†], Carlos López-Martínez[*], Roger Jové[†]*

[*]Remote Sensing Lab (RSLab), Department of Signal Theory and Communications (TSC)
Universitat Politècnica de Catalunya - Barcelona Tech (UPC)
Jordi Girona 1-3, Campus Nord, D4 Building, 08034, Barcelona, Spain
[†]Balam Ingeniería de Sistemas, SL

ABSTRACT

This paper provides a high level overview of a multi-frequency Ground-Based Synthetic Aperture Radar operating at X-, C-, L- and P-bands. The system core is implemented using a flexible high performance Software Defined Radio, aided by a custom radio-frequency front-end. The capabilities of the system are demonstrated by measuring dense time-series of a vegetated area. The benefits of lower frequencies appear as a significant increase in phase stability and coherences at P- and L-bands, which is explained by the increased vegetation penetration depth of these bands compared of C- and X-bands. It is concluded that multi-frequency measurements closely spaced in time are valuable and suggest new applications in vegetated areas.

***Index Terms*—** SAR, GBSAR, vegetation, multi-frequency

1. INTRODUCTION

Ground Based Synthetic Aperture Radar (GBSAR) has gained attention in the last years due to its real time measurement capability, needed for applications that involve fast-changing targets such as landslides or terrain subsidence. Most commercial GBSARs have a fixed hardware implementation and operate at a single frequency, usually at 17.3 GHz, within Ku-band [1]. This frequency allows high azimuth resolution with relatively short synthetic apertures, and it is adequate to sense areas consisting of bare soil. When the area is vegetated, strong decorrelation effects appear between images, and render them unusable for interferometry applications [2]. A possible way to overcome this limitation is to use lower frequencies that are less sensitive to vegetation due to their higher penetration depth, at the expense of a significant loss in azimuth resolution [3]. The main motivation to develop a multi-frequency GBSAR is to have a system that can adapt to the type of area under study. The prototype developed takes advantage of a high performance Software Defined Radio (SDR), that provides flexibility in signal generation and the processing of the received echo.

This research was partially funded by the Spanish Ministry of Economy and Competitiveness grant number DI-15-08147, the Catalan Ministry of Business and Knowledge grant number 2016 DI 012 and the Spanish Ministry of Science and Innovation grant number RTI2018-099008-B-C21.

2. SYSTEM DESCRIPTION

The implemented GBSAR system consists on a coherent radar unit that moves along a two meter long linear rail. The radar unit consists on a Software Defined Radio operating at up to 6 GHz and with 160 MHz of instantaneous bandwidth.. A custom compact external front-end assists in frequency extension up to X-band, amplification, filtering, providing analog Frequency Modulated Continuous Wave (FMCW) deramping and mitigating the transmit-receive leakage, a common problem of FMCW radars. The antennas consist on low-cost ultra-wideband aluminum Vivaldi elements for L-, C- and X-bands, and Printed Circuit Board (PCB) Log Periodic Dipole Array (LPDA) elements for P-band. In the results presented in this paper, the system operates at VV polarization, although it is prepared to simultaneously receive both vertical and horizontal polarizations. The system is designed to meet the following parameters:

- Bands: P(450MHz)/L(2.2 GHz)/C(5.4 Ghz)/X(10 GHz)
- Maximum range: 2 km
- Interferometric displacement accuracy: $<$1 mm
- Acquisition time per band: $<$10 s
- Range resolution: $>$1 m
- Aperture length: 2 m

The radar core movement is governed by a controller that drives a servo-motor, making use of the feedback of an encoder, ensuring an exact position at any given time. The controller receives commands from an external host through an Ethernet switch. The host computer is also in charge of communicating with the SDR, setting its configuration parameters and the ones of the external front-end, exerting control of the transmission and receiving the base-band samples for later processing. A picture of the final system is shown in Figure 1.

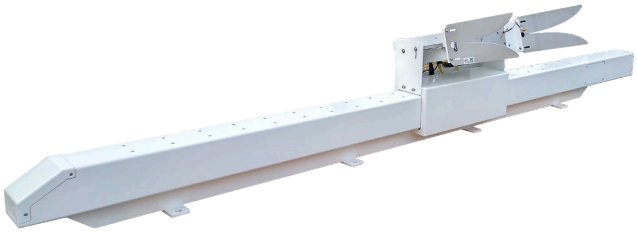

Fig. 1. Finished GBSAR system implementation.

3. FIRST MULTI-FREQUENCY TESTS

Extensive tests were carried out as part of the design cycle. In this paper, one of the test campaigns is shown. The objective of this test was to perform a set of time series at the four frequencies of a mostly vegetated scene, and to evaluate the differences between bands using either qualitative and quantitative assessments such as phase and amplitude stability and coherence.

The selected scene is located at Subirats castle, south Barcelona, Spain (41°24'57.9"N 1°48'59.2"E). The area consists on two vegetated hills separated by a road. The upper hill is vegetated mainly by mid-dense shrubland, with sparse rocky patches without vegetation, while the lower hill is more densely vegetated with a combination of shrubland and evergreen oaks. The difference in vegetation density is due to a wildfire that took place in 1994, which severely burnt the upper hill. Two Trihedral Corner Reflectors (TCR) were placed form validation and calibration. Figure 2 shows the scene from the radar point of vie along with delimited areas used later for coherence extraction, and an ortophoto of the scene can be seen in Figure 3.

The first amplitude image of the series at each band is shown in Figure 4. At C- and X-band the two TCRs are clearly visible, while at L- and P-band the their presence is less evident because either their Point Spread Function (PSF) lobes or their main lobes are buried under the surrounding scene energy. The road is clearly visible at X- and C-bands, mainly due to the high return of the rocky slopes and the metallic guard rails. An important observation is the strong target appearing at (20, 80) m [range, cross-range] at L- and P-bands, not present at X- nor C-band. This corresponds to a patch of rocky terrain buried below medium dense vegetation, and clearly indicates the penetration capability of the two lower bands.

In order to perform a quantitative assessment of the different bands, the coherence between the first acquisition and the other acquisitions was computed. There are in total 21 images for each band, taken 10 minutes apart.The areas chosen are depicted in Figure 2. The first area corresponds to the upper hill, comprising a range between 100 m and 130 m, just at the upper part of it. The second area is located at the same azimuth angle than the first one, but comprises a similarly vegetated area with flat terrain. Finally, the third area is a smaller area of the lower hill, with denser vegetation but containing various spots of very almost bare soil covered with a thin layer of vegetation.

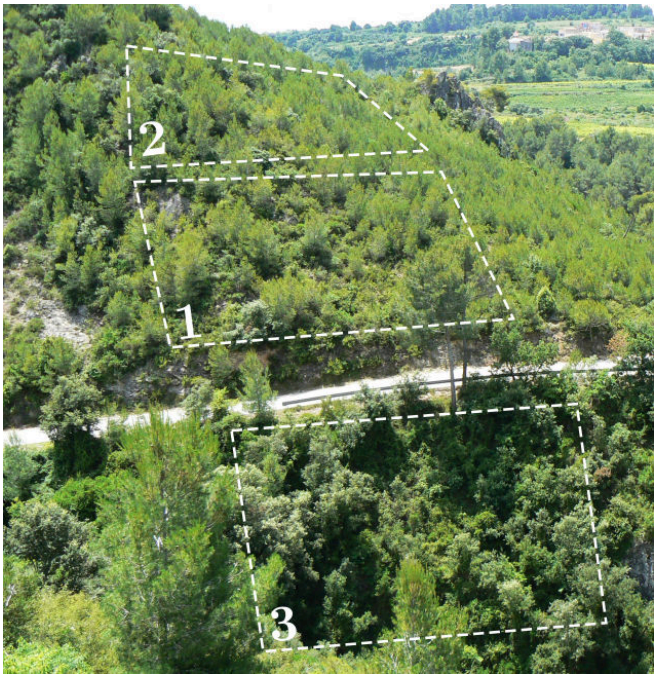

Fig. 2. Scene view from the GBSAR location and defined areas for coherence extraction.

Fig. 3. Ortophoto showing the scene, the location of the TCRs and the GBSAR location. Ortophoto credit: Institut Cartogràfic i Geològic d Catalunya.

Figure 5 shows the computed coherence magnitude for all areas. Starting with X-band, the first thing to note is the differing values for all three areas. The high coherence of Area 3 can be explained by the very low density vegetation spots

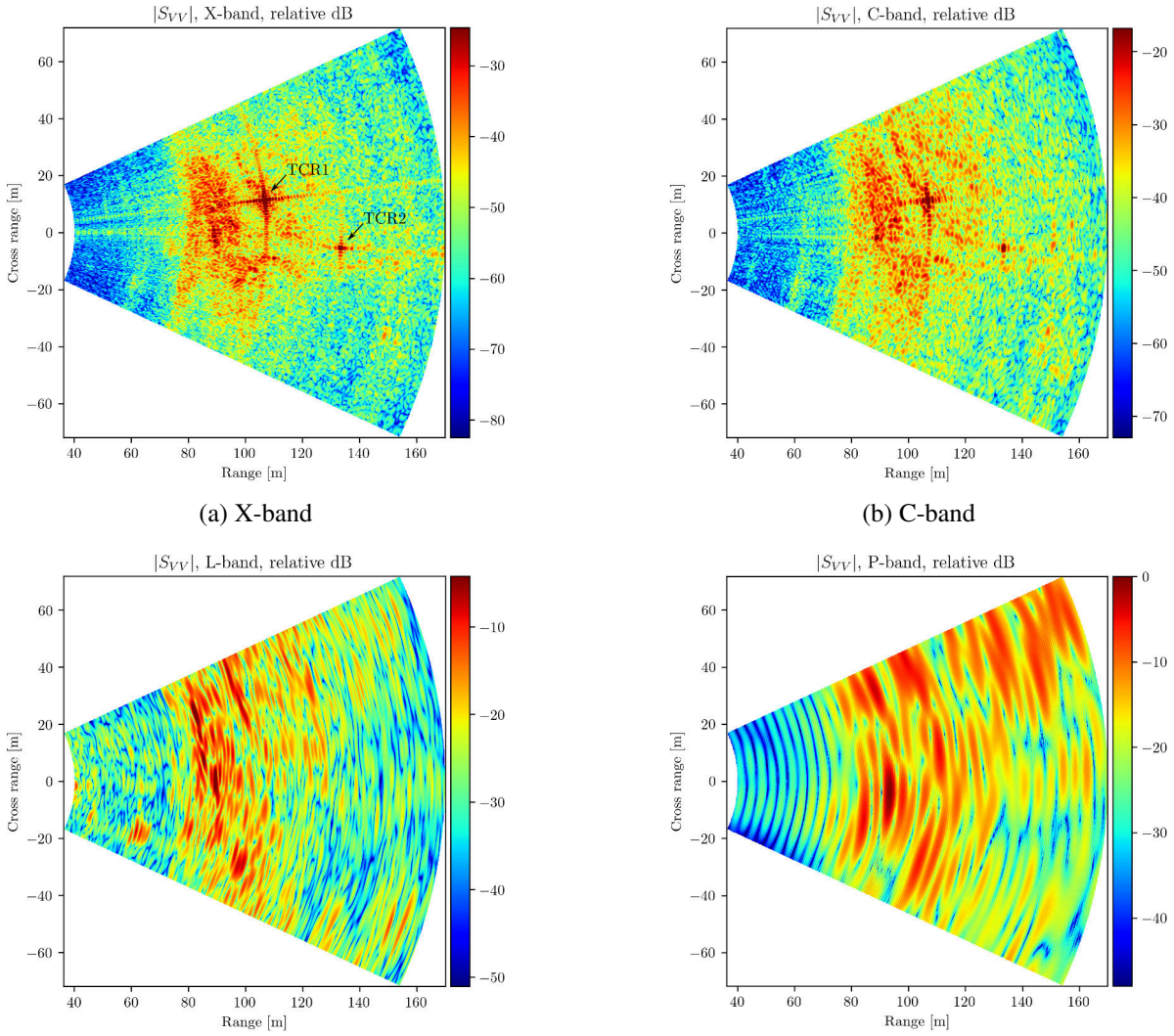

(a) X-band

(b) C-band

(c) L-band

(d) P-band

Fig. 4. Amplitude images at all bands

and the direct view of tree trunks, which are high coherence targets. The coherence of Area 1 is reduced due to the more consistent vegetation cover, while Area 2 presents a significantly lower coherence value. This low coherence value may be explained by the consistent and complete vegetation cover. At C-band, the coherence values are nearly identical, denoting a similar ability to X-band to penetrate medium-dense vegetation. At L-band, a drastic coherence increase is observed at all three areas, which is expected due to the significant enhancement in penetration depth. Finally, at P-band, a saturation in coherence is achieved at all three areas, proving the high insensitivity of this band to the type of vegetation present in the scene and the higher vegetation penetration. Also, a slow decrease in coherence is clearly observed at X-band, and in a lower degree at C-band, which may correlate with slow changes in atmospheric conditions or changes in some terrain parameters such as soil moisture.

Since the sampled coherence estimator is biased, especially for low coherence values [4], coherence values of Figure 5 have to be examined along with the estimated Equivalent Number of Looks (ENL) to certify that they are good unbiased estimates. An estimation of the ENLs for each are is shown in Table 1, which are sufficiently high to consider the biases negligible [4].

4. MAIN CONCLUSIONS

This paper has described a multi-frequency GBSAR system that operates at P-,L-,C- and X-bands and part of the results of a test campaign have been shown. The results indicate a

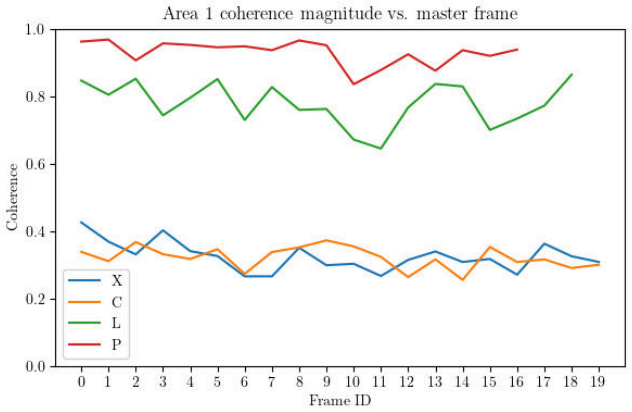

(a) Area 1

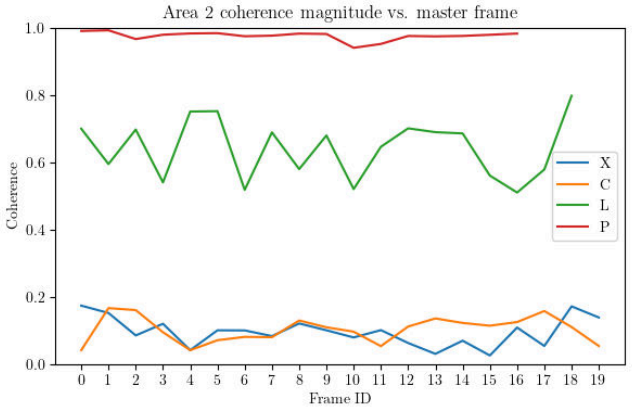

(b) Area 2

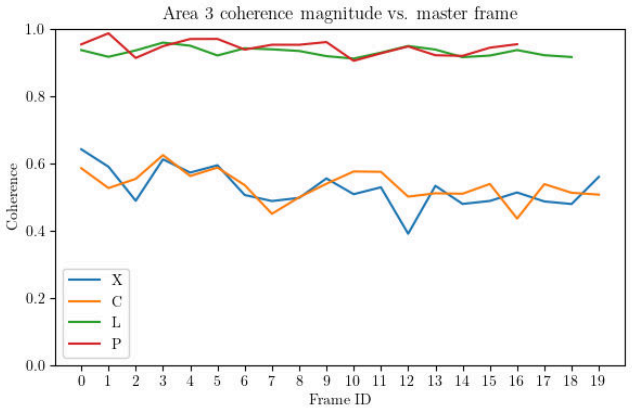

(c) Area 3

Fig. 5. Coherence magnitude for all areas and bands.

clear penetration capability of L- and C-bands in front of X- and C-bands, both by disclosing targets below vegetation and exhibiting a strong increase in coherence values in vegetated areas. The coherence values show that X- and C-bands have a very similar behaviour regarding coherence, and that there is a marked gap between the two lower frequency bands and the two higher ones. This gap suggest that it may be of interest performing the same kind of acquisitions at an intermediate band such as S-band. This band may represent a good compromise between azimuth resolution and coherence.

Table 1. Effective Number of Looks.

Frequency	X	C	L	P
Area 1	615	332	74	11
Area 2	811	438	97	15
Area 3	490	264	59	9

5. REFERENCES

[1] O. Monserrat, M. Crosetto, and G. Luzi, "A review of ground-based SAR interferometry for deformation measurement," *ISPRS Journal of Photogrammetry and Remote Sensing*, vol. 93, no. July, pp. 40–48, 2014.

[2] Guido Luzi, Massimiliano Pieraccini, Daniele Mecatti, Linhsia Noferini, Gabriele Guidi, Fabio Moia, and Carlo Atzeni, "Ground-based radar interferometry for landslides monitoring: Atmospheric and instrumental decorrelation sources on experimental data," *IEEE Transactions on Geoscience and Remote Sensing*, vol. 42, no. 11, pp. 2454–2466, 2004.

[3] E. Mougin, C. Proisy, G. Marty, F. Fromard, H. Puig, J. L. Betoulle, and J. P. Rudant, "Multifrequency and multipolarization radar backscattering from mangrove forests," *IEEE Transactions on Geoscience and Remote Sensing*, vol. 37, no. 1 PART 1, pp. 94–102, 1999.

[4] Ridha Touzi, Armand Lopes, Jérôme Bruniquel, and Paris W. Vachon, "Coherence estimation for SAR imagery," *IEEE Transactions on Geoscience and Remote Sensing*, vol. 37, no. 1 PART 1, pp. 135–149, 1999.